Preparation and Properties of the Single-Walled Carbon Nanotube/Cellulose Nanocomposites Using *N*-methylmorpholine-*N*-oxide Monohydrate

Dong-Hun Kim,[1] Soo-Young Park,[1] Junkyung Kim,[2] Min Park[2]

[1]*Department of Polymer Science, Kyungpook National University, 1370 Sangyuk-dong, Buk-gu, Daegu 702-701, Korea*
[2]*Korea Institute of Science and Technology, Hawolkog-Dong, Seongbuk-Gu, Seoul 136-791, Republic of Korea*

Received 19 October 2009; accepted 11 February 2010
DOI 10.1002/app.32247
Published online 12 May 2010 in Wiley InterScience (www.interscience.wiley.com).

ABSTRACT: Single-walled carbon nanotube (SWNT)/cellulose nanocomposite films were prepared using *N*-methylmorpholine-*N*-oxide (NMMO) monohydrate as a dispersing agent for the acid-treated SWNTs (A-SWNTs) as well as a cellulose solvent. The A-SWNTs were dispersed in both NMMO monohydrate and the nanocomposite film (as confirmed by scanning electron microscopy) because of the strong hydrogen bonds of the A-SWNTs with NMMO and cellulose. The mechanical properties, thermal properties, and electric conductivity of the nanocomposite films were improved by adding a small amount of the A-SWNTs to the cellulose. For example, by adding 1 wt % of the A-SWNTs to the cellulose, tensile strain at break point, Young's modulus, and toughness increased $\sim$ 5.4, $\sim$ 2.2, and $\sim$ 6 times, respectively, the degradation temperature increased to 9°C as compared with those of the pure cellulose film, and the electric conductivities at ϕ (the wt % of A-SWNTs in the composite) = 1 and 9 were 4.97×10^{-4} and 3.74×10^{-2} S/cm, respectively. Thus, the A-SWNT/cellulose nanocomposites are a promising material and can be used for many applications, such as toughened Lyocell fibers, transparent electrodes, and soforth. © 2010 Wiley Periodicals, Inc. J Appl Polym Sci 117: 3588–3594, 2010

Key words: lyocell; single-walled carbon nanotube; nanocomposite

INTRODUCTION

Cellulose is a renewable, biodegradable, and biocompatible and an almost inexhaustible source of raw materials that can be used to replace petrochemical compounds in many cases.[1–3] However, cellulose is difficult to process in a solution or melted state, because of its large proportion of intra- and intermolecular hydrogen bonds. Thus, the viscose process needs environmentally hazardous toxic chemicals, such as sulfuric acid (H_2SO_4) and carbon disulphide (CS_2). The "Lyocell" process made an industrial breakthrough as an environmentally friendly alternative to the viscose process, whereas cellulose is regenerated from a solution in *N*-methylmorpholine-*N*-oxide (NMMO) monohydrate, which is nontoxic and recoverable. Owing to its strong N—O dipole of NMMO, NMMO monohydrate can dissolve cellulose without the cell activation or derivatization. The Lyocell fiber has been known to have a higher strength (and modulus) but a lower stain at break point than the viscose fiber so that it has fibrillation tendency.[4] The long and thin crystallites of the Lyocell fiber have been considered as the origin of this fibrillation tendency.[5–7] Carbon nanotubes (CNTs) have attracted considerable attention as fillers in nanocomposites and for the development of electroconductive polymer materials with enhanced mechanical properties.[8–23] In particular, single-walled carbon nanotubes (SWNTs) have been expected to behave as a better ingredient than multi-walled carbon nanotubes (MWNTs) even at a low loading level because of their greater aspect ratio, high mechanical modulus, and good electroconductivity. Young's modulus of individual SWNTs is as large as $\sim$ 1 TPa,[24–27] which is even comparable with that of graphite (in-plane).[28] Furthermore, the electrical conductivity of bulk SWNTs is very high (10^2–10^3 S/cm).[29–31]

Several studies have been conducted on the CNT/cellulose nanocomposites as an alternative to making CNT-based nanocomposite sheets. Oya and Olino[32] have recently reported the electrically conductive SWNT/cellulose nanocomposite simply using the "washi" process by adding the SWNTs into the pulp suspension. However, a strong tendency of the

Correspondence to: S.-Y. Park (psy@knu.ac.kr).
Contract grant sponsor: Basic Science Research Program through National Research Foundation of Korea (NRF) funded by the Ministry of Education, Science and Technology; contract grant number: (2009-0073476).

SWNTs to form agglomerates led to the poor dispersion of the SWNTs in a cellulose matrix, resulting in rather poor mechanical and electroconductive properties.[33] Electrically conducting polymeric membranes were also prepared by incorporating MWNTs into bacterial cellulose pellicles.[34] However, the CNT dispersion in the cellulose matrix has still been of great concern. In the case of the nanocomposite preparation by solution-mixing, uniform CNT dispersion in solvents is still a big challenge as CNTs are amphiphobic, that is, they repel common polar and nonpolar solvents. During the past several years, the surface modification of CNTs by either noncovalent or covalent functionalization methods has been used to improve the solubility or dispersion of CNTs in solvents or polymers.[35] Recently, 1-Allyl-3-methylimidazolium chloride (AmimCl) [which is one of the room temperature ionic liquids (RTILs)], which is a desirable green solvent, have been reported as an effective and promising cellulose solvent.[36–44] However, this AmimCl is not commercially available.

In this article, a promising and emerging solvent for cellulose, NMMO monohydrate, was used for preparing the SWNT/cellulose nanocomposite film. NMMO monohydrate was used as a solvent for dispersing the acid-treated SWNTs as well as dissolving the cellulose. The mechanical, thermal, and electrical properties of the SWNT/cellulose nanocomposite film were reported in this article.

EXPERIMENTAL

Materials

Cellulose powder (Buckeye V-81 grade, number-averaged molecular weight (M_n) = 1200) and NMMO monohydrate (which was evaporated from 50 wt % aqueous solution of BASF© NMMO) were supplied by Kolon©. The SWNTs used in this study was purchased from Carbon Solution© (P2 grade). They were produced by an arc-discharge method and their carbonaceous purity was 70–90%. The SWNTs were further purified (functionalized) with acid-treatment in 2.6*M* nitric acid at 70°C for 24 h under reflux in the laboratory. The acid-treated SWNT was detonated as A-SWNT.

Nanocomposite preparation

NMMO monohydrate in a glass tube was heated to 95°C in an oil-bath, the SWNTs were added into the tube with different amounts, and the SWNTs in an NMMO solution were dispersed with an tip-type ultra-sonicator (Vibracell, VCX-750 700W/60Hz) for 7 h. The 5 wt % cellulose powders were then added into the SWNT/NMMO solution and mixed with a mechanical stirrer for 2 h. The dispersed nanocomposite dope was sonicated for 2 h, and finally degassed for 1 h to remove air with an aspirator in the dope. The viscous dope was poured on the glass plate and flattened into a film by drawing a glass bar over the plate. The gap between the glass bar and the plate was controlled by the thickness of the rolled tape on both end-edges of the glass bar. The film on the plate was immersed into a water container for a day to remove NMMO and dried with air in a sample holder.

Characterization

The micrographs of the osmium tetroxide (OsO_4)-coated surface of the SWNT/cellulose nanocomposite films were taken using a Hitachi S-4800 scanning electron microscope (SEM) with an accelerating voltage of 3 kV. The surface of film was plasma-etched with an oxygen plasma instrument (Yamato Scientific PC-103) to see the SWNTs in the film by removing the organic material on the surface. Fourier transform infrared (FTIR) spectra of the A-SWNTs and cellulose were taken with a FTIR spectrometer (FT/IR-620, Jasco) under vacuum. The samples were vacuum-dried for 1 day, mixed with KBr, and pressed into a 13-mm diameter pellet. The spectra were derived from 50 coadded interfergrams, which were obtained at a resolution of 1 cm^{-1}. Thermogravimetric analysis (TGA) thermograms of the nanocomposite films were taken on a TGA-50 (Shimadzu) from 150 to 500°C under nitrogen atmosphere with a scan rate of 10°C/min. The tensile properties of the SWNT/cellulose nanocomposite films were measured with an Instron 4465 (Instron) at 25°C. The length, width, and thickness were 30 mm, 10 mm, and 25 μm, respectively. The extension rate was set at 10 mm/min and the load cell was 5 kgf. The average and the standard deviation were calculated with 13 samples excluding the highest and lowest values. The standard deviation was shown in the error bar in the graphs. The conductivity of the SWNT/cellulose nanocomposite films was measured at an ambient temperature by a four-point probe method using a HMS-3000 (Ecopia). The dimensions of the samples were about 10 (length) × 10 (width) × ~ 0.025 (thickness) mm^3 and their ends were coated with an indium paste to ensure good electrical contact. The instrumental limit of the electrical conductivity is in the range of 10^3–10^{-6} S/cm. Transmittance measurement was performed using a UV/visible spectrophotometer (V-650, Jasco).

RESULTS AND DISCUSSION

The most prominent feature of NMMO is the highly polar N—O group with a dipole moment of

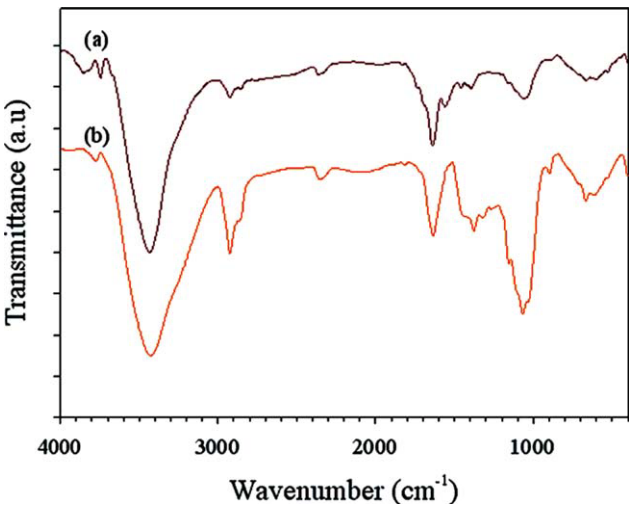

Figure 1 FTIR spectra of (a) the A-SWNTs and (b) the pure cellulose film. [Color figure can be viewed in the online issue, which is available at www.interscience.wiley.com.]

4.38 mD.[45] Because of the high polarity of the N—O bond, the oxygen of the N—O group in NMMO is able to form one or two hydrogen bonds with partners containing hydroxyl (or carboxylic acid) groups. Figure 1 shows the IR spectra of the A-SWNTs and the pure cellulose films. Both exhibit the hydroxyl bands at 1700, 1000–1200, and 3500–3600 cm^{-1} and the carboxylic acid band at 1720–1650 cm^{-1}. The hydroxyl and carboxylic acid groups of the A-SWNT are capable of making hydrogen bonds with the N—O groups of NMMO. These hydrogen bonds would facilitate dispersion of the A-SWNTs in NMMO. The hydroxyl and carboxylic acid groups of the A-SWNTs can also interact strongly with those of the cellulose in the composite films (after coagulation), which may increase not only the dispersion of the A-SWNTs (in the composite film) but also mechanical properties of the composite films.

Figure 2(a,b) are the photographic images of the 1 wt % A-SWNT solution in NMMO after mechanical stirring without sonication and with sonication for 7 h, respectively. The solution without sonication was transparent and the grained particles were visible in the solution [Fig. 2(a)], whereas the homogenous and well-dispersed black A-SWNT solution was obtained with sonication [Fig. 2(b)], indicating that the mechanical mixing was not enough and sonication was necessary to disperse the A-SWNTs in the NMMO solution. Figure 2(c) shows the 1 wt % nanocomposite film in the sample holder after drying at room temperature for 24 h. The film was in good shape and was transparent for the low-SWNT content films (transparency will be discussed later). The mechanical and thermal properties, transmittance, and electrical conductivity were studied with these films.

Figure 3(a) shows the stress versus strain curves of the 0, 1, and 2 wt % nanocomposite films as examples. Stress linearly increased as strain increased before yield stress. The images of the inset in Figure 3(a) are photographs during the tensile measurement of the 1 wt % nanocomposite film at 0 and 20% strain. The shape of film was not distorted without any pleat although the film was extended 20%. This extension is a significant achievement if the cellulose low extension characteristic is considered. Figure 3(b–d) show tensile strain at break point, tensile stress at break point and Young's modulus, and toughness as a function of the A-SWNT content (ϕ in wt %), respectively. Tensile stress at break point, Young's modulus, tensile strain at break point, and toughness had a maximum at $\phi = \sim 1$.

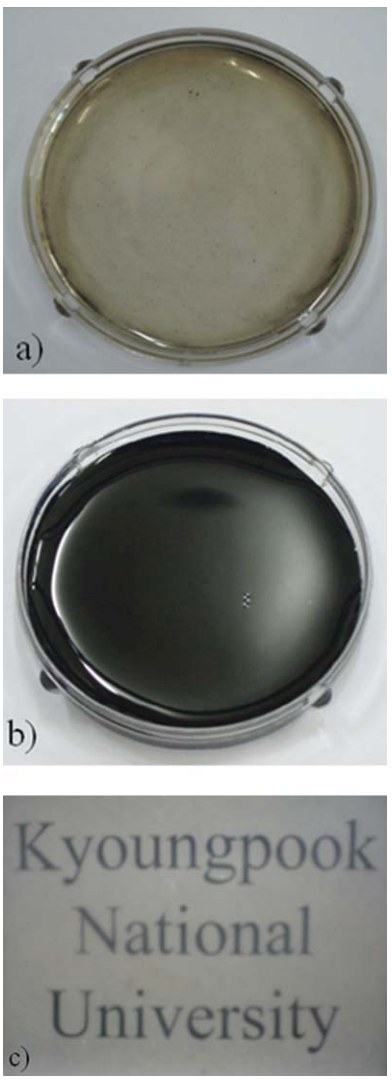

Figure 2 Photographic images of the 1 wt % SWNTs solution in NMMO (a) before and (b) after sonication for 7 h, and (c) the 1 wt % nanocomposite film in the frame after drying at room temperature for 24 h. [Color figure can be viewed in the online issue, which is available at www.interscience.wiley.com.]

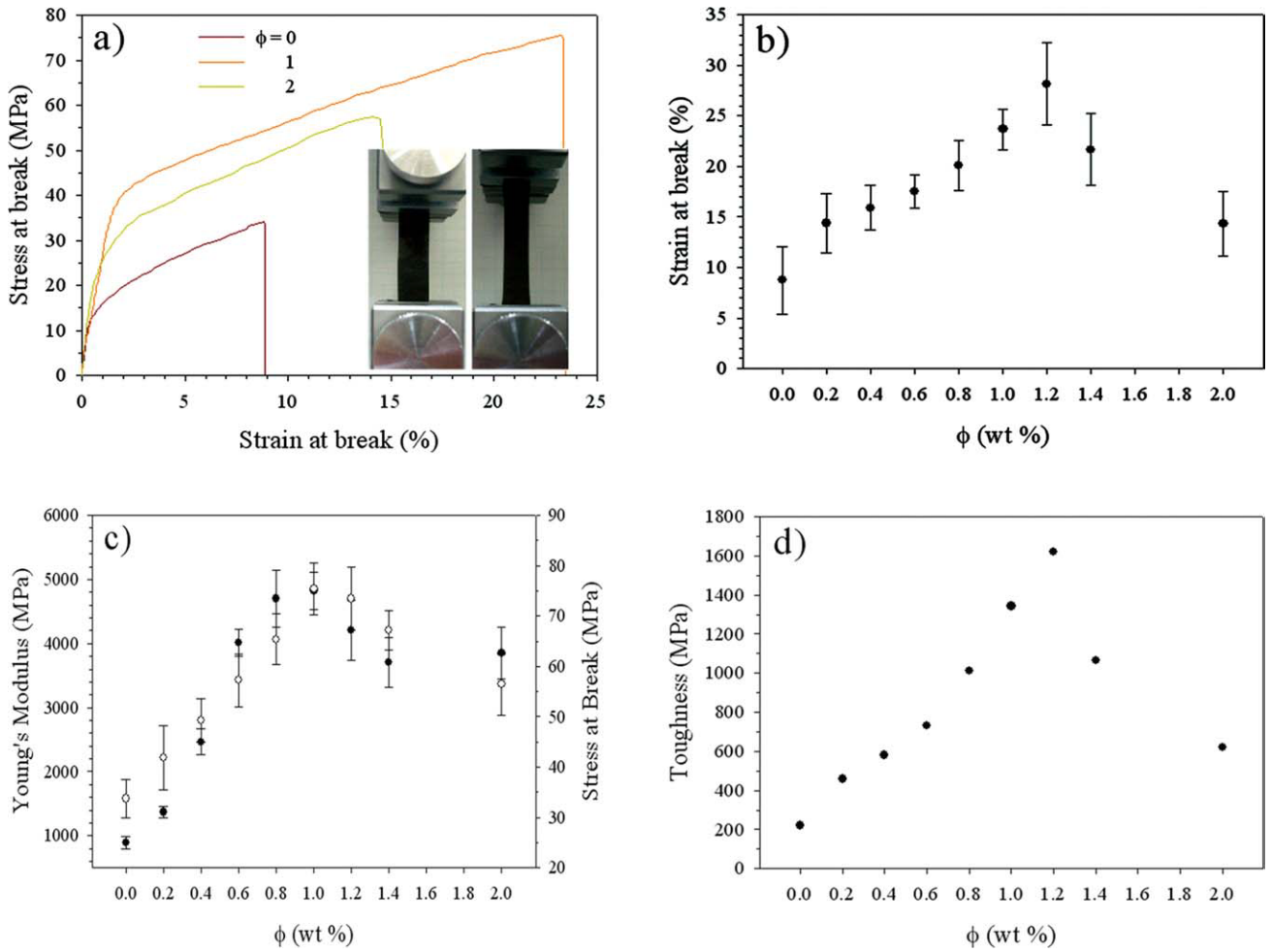

Figure 3 (a) Tensile stress and strain curves, (b) tensile strain at break point, (c) tensile stress at break point (○) and Young's moduli (●), and (d) toughness of the nanocomposite films as a function of the ϕ. [Color figure can be viewed in the online issue, which is available at www.interscience.wiley.com.]

Tensile strain at break point and Young's modulus increased ~ 5.4 and ~ 2.2 times by adding 1 wt % A-SWNT, respectively. Toughness at $\phi = 1$ is 1343 MPa, which is ~ 6 times higher than that of the pure cellulose (220 MPa). Lyocell has been known to be more brittle than viscose Rayon. The increase of toughness may be due to the hydrogen-bond interactions between the A-SWNT and the cellulose. However, the decrease of the mechanical properties after $\phi = 1$ may be related to the poor dispersion of the A-SWNTs through percolation of the A-SWNTs, which will be discussed in the later section.

Figure 4 shows the SEM micrographs of the surface of the plasma-etched films at $\phi = 0$, 1, and 2. The surface of the plasma-etched film at $\phi = 1$ [Fig. 4(b)] shows the well-dispersed SWNTs. The white parts (including gradules) were due to the ashes of the burned cellulose, which was confirmed with the SEM micrograph of the pure cellulose film [Fig. 4(a)]. SWNT has a diameter of ~ 2 nm and exists in bundles measuring almost 20–40 nm in nanocomposite films. The A-SWNTs at $\phi = 2$ were entangled in several parts and were not well dispersed when compared with the nanocomposite film at $\phi = 1$. The poorly dispersed A-SWNTs at $\phi = 2$ may cause the deterioration of the mechanical properties in Figure 3. Figure 4(d) shows the cracked surfaces at $\phi = 1$. The SWNTs protruded from the cracked surface and were surrounded by the cellulose matrix at the bottom of the protruded SWNT from matrix, indicating that the strong interactions by hydrogen bonding existed between the SWNTs and the cellulose matrix. The well-dispersed SWNTs and strong interactions between the SWNTs and the cellulose improved mechanical properties of the composite films at low loading of SWNTs.

Figure 5(a,b) shows the TGA thermograms and their first derivatives of the completely dried nanocomposite films in vacuum oven, respectively. The peak position of the first derivatives [Fig. 5(b)] increased as the ϕ increased; the peak positions of the first derivative at $\phi = 0$ and 1 were 329 and 338°C, respectively. The increase of the degradation temperature indicates that the incorporation of

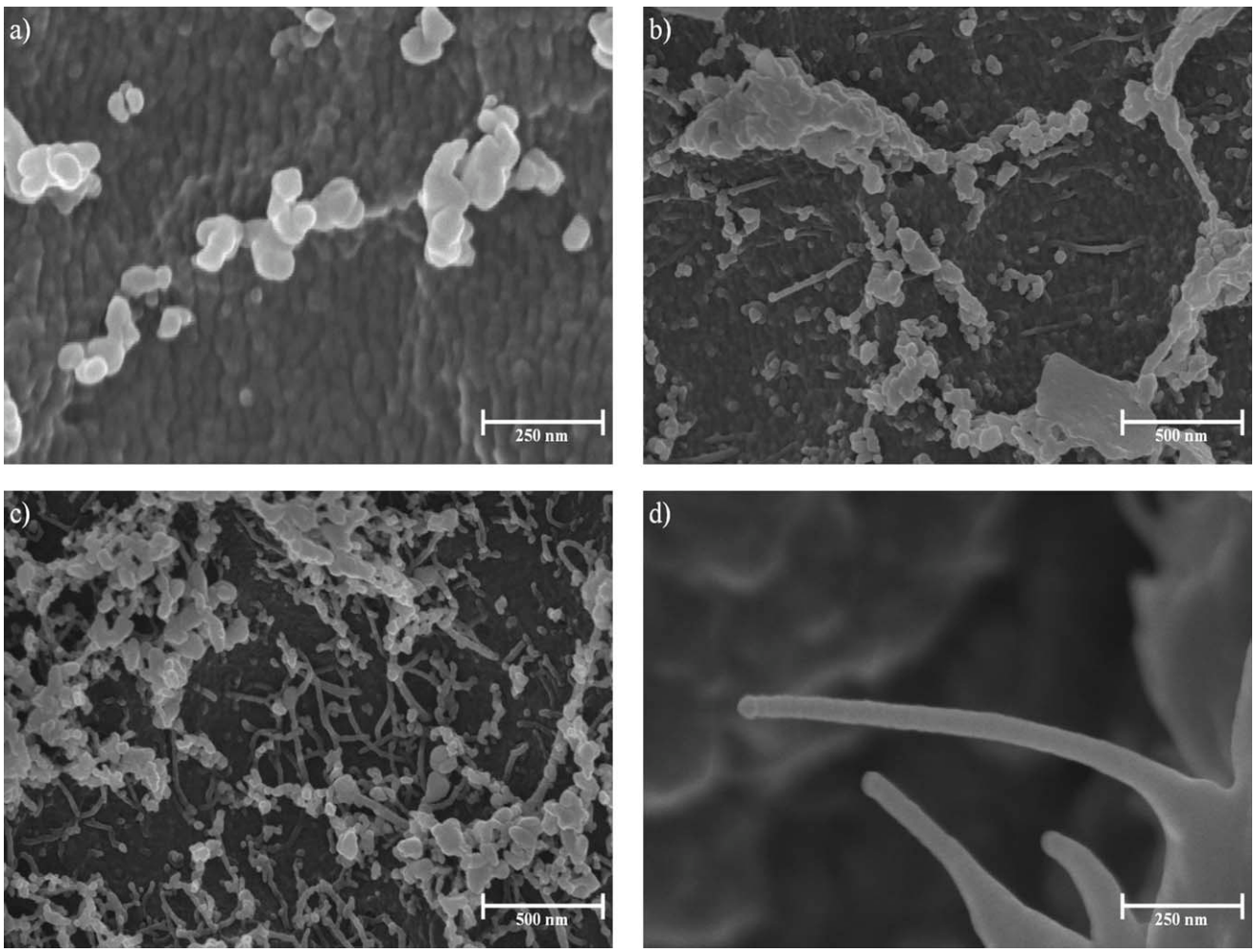

Figure 4 SEM micrographs of the surface of the plasma-etched films at ϕ = (a) 0, (b) 1, and (c) 2, and (d) the cracked surfaces at $\phi = 1$.

SWNT into the cellulose exerts a thermal stabilizing effect in the composite. Figure 5(c) shows the residues of the TGA thermograms at 500°C with respective to ϕ. The residue increased as the ϕ increased; the residues increased from 24.7 to 26.9 wt % by adding 1 wt % A-SWNTs. The slope changed at $\phi = 1$; the slope was 2.35 and 0.62 before and after $\phi = 1$, respectively. The slope >1 suggests that the materials were carbonized more than the input of the SWNTs probably because of the large interface (between SWNTs and cellulose), which could be nuclei for carbonization. The slope <1 after $\phi = 1$ also suggests that SWNTs were overlapped because of the percolation of SWNTs in the matrix. Other properties such as mechanical properties and electrical conductivity (which will be discussed later) had maximum at $\phi = 1$ indicating that the percolation threshold might be 1 wt % in this system.

Figure 6(a,b) show the transmittances of the nanocomposite films as a function of wavelength [Fig. 6(a)] and those at 550 nm as a function of the ϕ [Fig. 6(b)]. The transmittance continuously decreased as the wavelength and the ϕ increased. Transmittances of the films at $\phi = 0.2$, 0.4 and 0.6 wt % were 92.6, 86.4 and 81.4% at 550 nm, respectively. This high transmittance indicates that the A-SWNTs were well dispersed in the nanocomposite film. Figure 6(c) shows the electrical conductivities of the nanocomposite films as a function of the ϕ. Electrical conductivity increased as the ϕ increased. The nanocomposite films were conductive even at $\phi = 0.2$. The conductivity levels were 4.97×10^{-4}, 4.39×10^{-3}, and 3.74×10^{-2} S/cm at $\phi = 1$, 5, and 9. This high conductivity might be due to the well-dispersed A-SWNT in cellulose and would increase more if better dispersion conditions were found. Transparent conducting organic films have been widely used in the applications of electrodes of capacitors and photodiodes,[46] antistatic coating,[47] electrochromic windows,[48] field effect transistors,[49] and hole transport materials.[50,51] Thus, this Lyocell/SWNT nanocomposite film may be one of the good candidates for these applications. In summary, the cellulose (which is a renewable, biodegradable, and

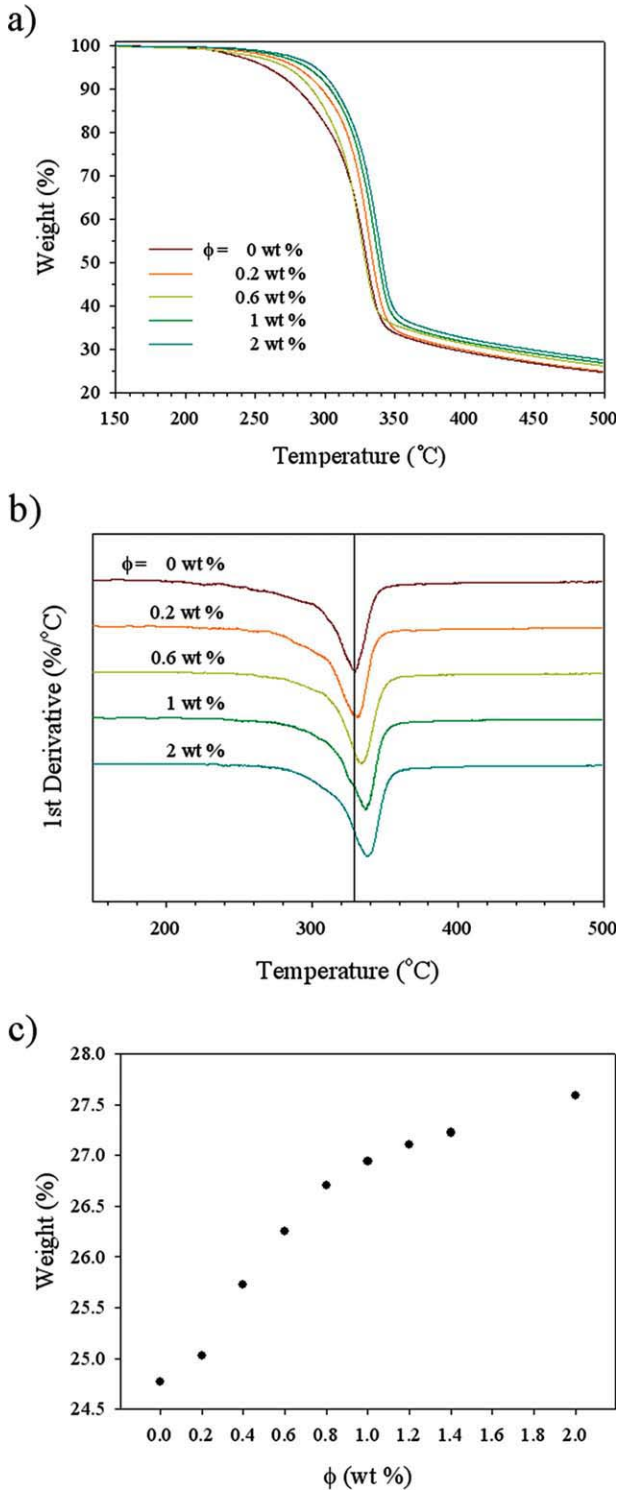

Figure 5 (a) TGA thermograms of the nanocomposite films, (b) their first derivatives with respect to temperature, and (c) their residue at 500°C with respect to ϕ. [Color figure can be viewed in the online issue, which is available at www.interscience.wiley.com.]

biocompatible and an almost inexhaustible source of raw materials that can be used to replace petrochemical compounds in many cases) was soluble in the environmentally-friendly NMMO, which could disperse A-SWNT, too. This unique combination of solubility and dispersity of NMMO makes the A-SWNT/cellulose conductive at lower loading of SWNT and tough because of the hydrogen-bond interactions between the A-SWNT and the cellulose.

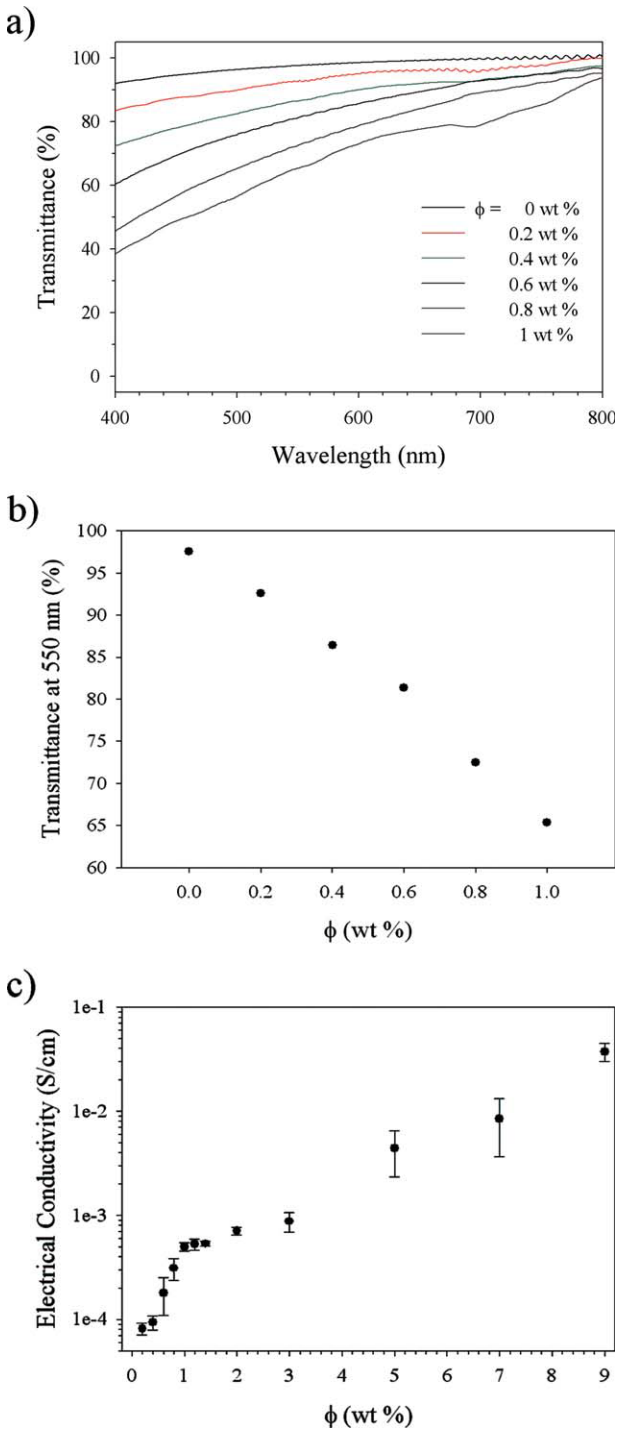

Figure 6 (a) The transmittances of the nanocomposite films as a function of wavelength with the different ϕs, (b) those at 550 nm as a function of the ϕ, and (c) electrical conductivities of the nanocomposite films as a function of the ϕ. [Color figure can be viewed in the online issue, which is available at www.interscience.wiley.com.]

CONCLUSIONS

NMMO monohydrate was used to make toughened, electro-conducting, and transparent SWNT/cellulose nanocomposite films. NMMO monohydrate was a good dispersing agent for A-SWNTs in the nanocomposite. The A-SWNT/cellulose nanocomposite films showed increased mechanical and thermal properties. For example, by adding 1 wt % of the A-SWNTs to the cellulose, tensile strain at break point, Young's modulus, and toughness increased ~ 5.4, ~ 2.2, and ~ 6 times, respectively, and the degradation temperature increased to 9°C with compared with those of the pure cellulose film. The increase in toughness is a significant achievement in industrial applications of Lyocell fiber because the brittleness of Lyocell fiber is one of the few disadvantageous properties. The conductivities of the nanocomposite films increased as the ϕ increased; the conductivities at $\phi = 1$ and 9 were 4.97×10^{-4} and 3.74×10^{-2} S/cm, respectively. The nanocomposite films were also transparent at the low ϕs; the UV transmittances at $\phi = 0.2$, 0.4, and 0.6 were 92.6, 86.4 and 81.4%, respectively. Thus, the SWNT/cellulose nanocomposites (which were prepared by the so-called "Lyocell" process) were a promising material in all properties studied in this article and can be used for many applications, such as toughened Lyocell fibers, transparent electrodes, and soforth.

References

1. Klemm, D.; Heublein, B.; Fink, H. P.; Bohn, A. Angew Chem Int Ed 2005, 44, 3358.
2. Klemm, D.; Schmauder, H. P.; Heinze, T. In Biopolymers; Vandamme, E., De Beats, S., Steinbchel, A., Eds.; Wiley-VCH: Weinheim, 2002; Vol. 6, p 290.
3. Kaplan, D. L. In Biopolymers from Renewable Resources; Kaplan, D. L., Ed.; Springer: Berlin, 1998.
4. Fink, H. P.; Weigel, P.; Purz, H. J.; Ganster, J. Prog Polym Sci 2001, 1473.
5. Chanzy, H.; Dube, M.; Marchessatult, R. H. J Polym Sci Lett Ed 1979, 17, 219.
6. Dub, M.; Blackwell, R. H. Proceedings of the International Dissolving and Speciality Pulps Conference; Tappi Press: Boston, 1983.
7. Fink, H. P.; Weigel, P.; Purz, H. J.; Ganster, J. Prog Polym Sci 2001, 26, 1473.
8. Iijima, S. Nature 1991, 354, 56.
9. Iijima, S.; Ichihashi, T. Nature 1993, 363, 603.
10. Dresselhaus, M. S.; Dresselhaus, G.; Avouris, P., Eds.; Springer: Berlin, 2001.
11. Baughman, R. H.; Zakhidov, A. A.; De Heer, W. A. Science 2002, 297, 787.
12. Calvert, P. Nature 1999, 399, 210.
13. Ajayan, P. M. Chem Rev 1999, 99, 1787.
14. Shaffer, M. S. P.; Windle, A. H. Adv Mater 1999, 11, 937.
15. Ajayan, P. M.; Schadler, L. S.; Giannaris, C.; Rubio, A. Adv Mater 2000, 12, 750.
16. Dalton, A. B.; Stephan, C.; Coleman, J. N.; Mccarthy, B.; Ajayan, P. M.; Lefrant, S.; Bernier, P.; Blau, W. J.; Byrne, H. J. J Phys Chem B 2000, 104, 10012.
17. Fisher, F. T.; Bradshaw, R. D.; Brinson, L. C. Appl Phys Lett 2002, 80, 4647.
18. Kymakis, E.; Alexandou, I.; Amaratunga, G. A. J. Synth Met 2002, 127, 59.
19. Du, F. M.; Fischer, J. E.; Winey, K. I. J Polym Sci Part B Polym Phys 2003, 41, 3333.
20. Ramasubramaniam, R.; Chen, J.; Liu, H. Appl Phys Lett 2003, 83, 2928.
21. Sreekumar, T. V.; Liu, T.; Min, B. G.; Guo, H.; Kumar, S.; Hauge, R. H.; Smalley, R. E. Adv Mater 2004, 16, 58.
22. Coleman, J. N.; Cadek, M.; Blake, R.; Nicolosi, V.; Ryan, K. P.; Belton, C.; Fonseca, A.; Nagy, J. B.; Guńko, Y. K.; Blau, W. J. Adv Funct Mater 2004, 14, 791.
23. Gao, J.; Itkis, M. E.; Yu, A.; Bekyarova, E.; Zhao, B.; Haddon, R. C. J Am Chem Soc 2005, 127, 3847.
24. Treacy, M. M. J.; Ebbesen, T. W.; Gibson, J. M. Nature 1996, 381, 678.
25. Krishnan, A.; Dujardin, E.; Ebbesen, T. W.; Yianilos, P. N.; Treacy, M. M. J. Phys Rev B 1998, 58, 14013.
26. Salvetat, J. P.; Briggs, G. A. D.; Bonard, J. M.; Bacsa, R. R.; Kulik, A. J.; Stöckli, T.; Burnham, N. A.; Forr, K. L. Phys Rev Lett 1999, 82, 944.
27. Yu, M. F.; Files, B. S.; Arepalli, S.; Ruoff, R. S. Phys Rev Lett 2000, 84, 5552.
28. Kelly, B. T. Phys Graphite, Appl Sci 1981,
29. Fischer, J. E.; Dai, H.; Thess, A.; Lee, R.; Hanjani, N. M.; Dehaas, D. L.; Smalley, R. E. Phys Rev B 1997, 55, R4921.
30. Kaiser, A. B.; Dlsberg, G.; Roth, S. Phys Rev B 1998, 57, 1418.
31. Hilt, O.; Brom, H. B.; Ahlskog, M. Phys Rev B 2000, 61, R5129.
32. Oya, T.; Ogino, T. Carbon 2008, 46, 169.
33. Thess, A.; Lee, R.; Nikolaev, P.; Dai, H.; Petit, P.; Robert, J.; Xu, C.; Lee, Y. H.; Kim, S. G.; Rinzler, A. G.; Colbert, D. T.; Scuseria, G. E.; Tomanek, D.; Fischer, J. E.; Smalley, R. E. Science 1996, 273, 483.
34. Yoon, S. H.; Jin, H.-J.; Kook, M.-C.; Pyun, Y. R. Biomacromolecules 2006, 7, 1280.
35. Andrews, R.; Weisenberger, M. C.; Curr, O. Solid State Mater Sci 2004, 8, 31.
36. Swatloski, R. P.; Spear, S. K.; Holbrey, J. D.; Rogers, R. D. J. Am Chem Soc 2002, 124, 4974.
37. Turner, M. B.; Spear, S. K.; Holbrey, J. D.; Rogers, R. D. Biomacromolecules 2004, 5, 1379.
38. Heinze, T.; Schwikal, K.; Barthel, S. Macromol Biosci 2005, 5, 520.
39. Wu, J.; Zhang, J.; Zhang, H.; He, J. S.; Ren, Q.; Guo, M. L. Biomacromolecules 2004, 5, 266.
40. Zhang, H.; Wu, J.; Zhang, J.; He, J. S. Macromolecules 2005, 38, 8272.
41. Fukushima, T.; Kosaka, A.; Ishimura, Y.; Yamamoto, T.; Takigawa, T.; Ishii, N.; Aida, T. Science 2003, 300, 2072.
42. Whitten, P. G.; Spinks, G. M.; Wallace, G. G. Carbon 2005, 43, 1891.
43. Fukushima, T.; Kosaka, A.; Yamamoto, Y.; Aimiya, T.; Notazawa, S.; Takigawa, T.; Inabe, T.; Aida, T. Small 2006, 2, 554.
44. Bellayer, S.; Gilman, J. W.; Eidelman, N.; Bourbigot, S.; Flambard, X.; Fox, D. M.; De, Long, H. C.; Trulove, P. C. Adv Funct Mater 2005, 15, 910.
45. Linton, E. P. J Am Chem Soc 1940, 62, 1945.
46. Groenendaal, L.; Jonas, F.; Freitag, D.; Pielartzik, H.; Reynolds, J. R. Adv Mater 2000, 12, 481.
47. Dkhissi, A.; Louwet, F.; Groenendaal, L.; Beljonne, D.; Lazzaroni, R.; Bredas, J. L. Chem Phys Lett 2002, 359, 466.
48. Heuer, H. W.; Wehrmann, R.; Kirchmeyer, S. Adv Funct Mater 2002, 12, 89.
49. Epstein, A. J.; Hsu, F.-C.h; Chiou, N.-R.; Prigodin, V. N. Curr Appl Phys 2002, 2, 339.
50. Pei, Q.; Zuccafrello, G.; Ahlskog, M.; Inganas, O. Polymer 1994, 35, 1347.
51. Jonas, F.; Morrison, T. Synth Met 1997, 85, 1397.